Efficiency Measurements on the CEBAF Hall A VDCs

by

Craig Leathers

Submitted to the Department of Physics
in partial fulfillment of the requirements for the degree of

Bachelor of Science in Physics

at the

MASSACHUSETTS INSTITUTE OF TECHNOLOGY

May 1996

Author .....
Department of Physics
May 20, 1996

Certified by .....
William Bertozzi
Thesis Supervisor, Department of Physics
Thesis Supervisor

Accepted by .....
June L. Matthews
Senior Thesis Coordinator, Department of Physics

Efficiency Measurements on the CEBAF Hall A VDCs

by

Craig Leathers

Submitted to the Department of Physics
on May 20, 1996, in partial fulfillment of the
requirements for the degree of
Bachelor of Science in Physics

Abstract

Thesis Supervisor: William Bertozzi
Title: Thesis Supervisor, Department of Physics

Efficiency Measurements on the CEBAF Hall A VDCs

by

Craig Leathers

Submitted to the Department of Physics
on May 20, 1996, in partial fulfillment of the
requirements for the degree of
Bachelor of Science in Physics

Abstract

The nuclear interactions group at MIT has been constructing vertical drift chambers (VDCs) for hall A of the Continuous Electron Beam Accelerator Facility (CEBAF) in Newport News, Virginia. The VDCs are used to detect the position at which a particle crosses it with very high accuracy. The chambers consist of two sets of parallel anode wires surrounded by an ionizable gas and two cathode planes. Efficiency measurements were taken with a 62% argon, 38% ethane gas mixture. Generally, an efficiency plateau of 99% was reached when the threshold voltage on the cards was set above the noise.

Thesis Supervisor: William Bertozzi
Title: Thesis Supervisor, Department of Physics

Contents

Chapter 1

Introduction

A vertical drift chamber (VDC) is a particle detector which measures the position where a charged particle crossed a given plane. It consists of many wires defining this plane. Each wire amplifies the signal of the track by an avalanche near the wire. In some drift chambers the avalanche operates in a proportional regime. The drifting of the primary ionization electrons to the avalanche or sense wire is used to interpolate the position of the track between the wires. The Nuclear Interactions Group at MIT has built five such chambers for use in the Continuous Beam Accelerator Facility (CEBAF), which is being constructed in Newport News, Virginia.

The avalanche process in a VDC is a critical element in its suitability for use as a particle detector. This process can be understood by considering the simple example of a classic cylindrical-geometry proportional counter. A proportional counter includes an anode wire and a surrounding cathode cylinder, and a gas between the two. When a particle is to be detected, it traverses the gas volume, ionizing it. The resulting electrons then drift to the anode wire. From Gauss's law, the field around the cylinder is

$$\mathbf{E} = \frac{Q}{r\epsilon 2\pi}, \tag{1.1}$$

where Q is the charge per unit length on the anode, r is the distance from the center of the anode, and an infinite length for the cylinder is assumed. From the above equation it is apparent that the field is very high at very small distances from the anode. This

high field causes the drifting electrons to acquire enough energy between collisions to ionize further atoms, liberating more electrons which cause more ionizations, allowing the original electrons to multiply in an 'avalanche' toward the anode. If the counter is operated in the correct voltage range, there will be enough electrons and ions for a detectable signal to be used to indicate that a particle crossed the detector volume. The signal might be proportional to the number of original electrons ionized by the passing particle, hence the name proportional counter. The condition of proportionality is not necessary to the operation of the VDCs described here, which have high gain. In these chambers, timing the electrons' drift to the wires is more important.

Multiwire proportional chambers were first developed by Charpak in the 1960s. It had been believed that there was no point in building a detector with more than one wire in the gas volume, because capacitive coupling would thwart any attempt to find which wires were near the ionizations caused by the particle. However, the electrons that participate in the avalanche resulted from the ionizations of neutral atoms, thus positive ions are left behind. Charpak realized that the positive induced signals from the ions compensate for the capacitive coupling effects. Capacitive coupling would induce a negative charge on neighboring wires, but it would be canceled by the charge from the positive ions resulting from the avalanche. Thus there is very little signal on a wire from the avalanche on a neighbor.[1]

The first multiwire proportional chambers were horizontal drift chambers (HDCs). They used both cathode and anode wires in the gas volume, and the electrons would drift to the anode wires. The chambers constructed for use at CEBAF are vertical drift chambers (VDCs). They use only anode wires, with cathode planes of gold coated mylar.

In the experiments done at CEBAF, the products of a scattering event are guided toward the VDCs by the spectrometer's dipole magnets. Accurate measurements of the particle's trajectory at the spectrometer's focal plane can be used to reconstruct important information about the detected particle, such as its momentum and the

[1]Konrad Kleinknecht, *Detectors for Particle Radiation,* Cambridge University Press, New York, 1986, p. 67.

direction with which it exited the scattering target. One VDC is placed at the focal plane, and measures accurately the position at which the particle crosses the focal plane. However, an accurate reconstruction of the particle's momentum vector at the target location requires measurement of not only the focal plane position, but also the particle's direction when crossing the focal plane. To obtain a precise measurement of the angle of a track, two chambers must be used, one on top of the other. Comparing the location at which a particle crosses the first detector with the location the particle crosses the second detector can give the angle with which the particle crossed the two chambers. CEBAF will use four drift chambers, in two sets of two. When in use, the particles will be crossing the chamber at an angle of roughly 45 degrees.

Chapter two of this thesis includes descriptions of the operation and the gain from the gas of the chambers, and an equation for the current pulses obtained. Chapter three containes details of the construction of the chambers. The results of experiments performed at CEBAF to obtain the chamber efficiency are included in chapter four, as well as a comparison between the gain that should result in the efficiency that was measured, and the gain that should result according to a described model. The efficiency is the number of times a wire gave a sufficiently large current pulse when a particle crossed the gas volume close to the wire.

I would like to thank my thesis advisor Prof. William Bertozzi for general advice. I would especially like to thank postdoctoral researcher Dr. Jeff Templon for frequent and detailed interactions regarding this work. I would like to thank Dr. Bogdan Wojtsekhowski, who supervised the data collection at CEBAF. I would also like to thank Risa Wechsler, who occasionally provided me with data from the Garfield analysis program. I would also like to thank Nilanga Liyanage for supervision during construction of the VDCs, and general advice.

Chapter 2

Operation

The vertical drift chambers (VDCs) operate as a series of proportional counters. The electric field in the immediate vicinity of the sense wire follows the pattern of an electric field inside a cylindrical proportional counter, so the gain characteristics of a proportional counter match those of a VDC when the drifting electrons reach the avalanche region. Before the avalanche region, the electrons gain so little energy between collisions that ionizations are effectively eliminated and the electrons settle into a constant drift velocity. When the electron gets close enough to the wire, it reaches a region where the field is stronger, and the electron gains enough energy to ionize more atoms and an electron multiplication avalanche occurs, as in a proportional counter.

When a charged particle passes through the chamber, the gas along its track will be ionized. The electrons resulting from these ionizations follow field lines to the anode wires, as illustrated in figure 2-1. The large picture on the left in the figure is an illustration of the particle's path through the gas, and the electric field lines caused by the voltage difference and geometry of the cathode planes and anode wires. The smaller graph in the upper right is a schematic diagram of the larger picture, with the wire position indicated horizontally and the distance to the track indicated vertically. This distance is measured perpendicularly to the wire plane and through each wire. The similar graph at the lower right of the figure shows the wire position on the horizontal axis, and the drift times on the vertical axis. Using these times, an

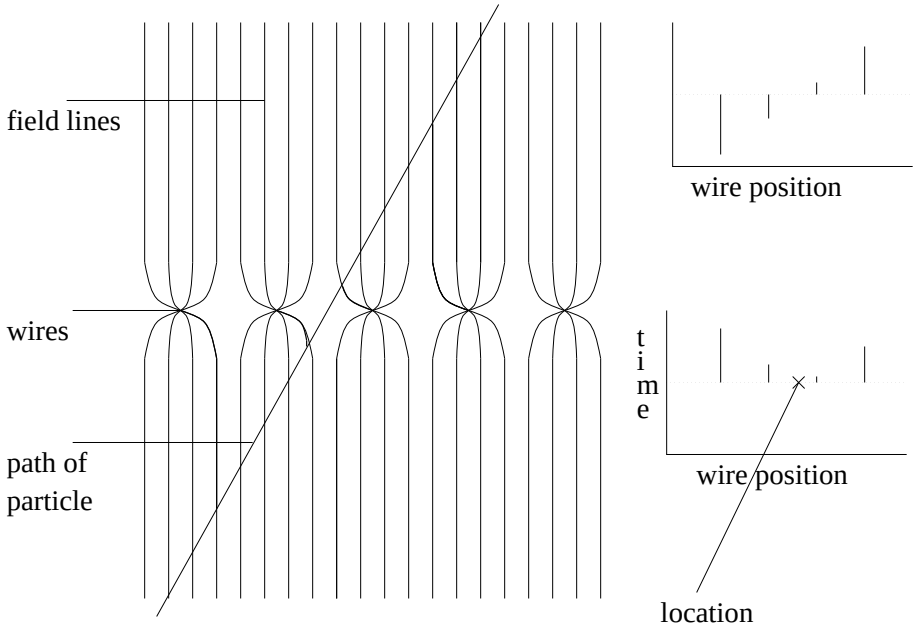

Figure 2-1: Electric Field and Drift Time vs. Position Graphs

estimate of the position at which the particle crossed the chamber can be obtained. The time will be proportional to the path's vertical distance (defined above) from that particular wire, plus a constant offset to take into account the drift line curvature and the strong nonlinear region of the field near the anode wire, which is where avalanche multiplication takes place. The information of the drift times can be used to accurately determine where the particle crossed the plane of the wire.

Noble gases are used in the gas mixture because they are favorable in the formation of an avalanche, compared to polyatomic gases. Argon is commonly used because it is cheaper than Xenon and Krypton. However, when noble gases are used, care must be taken because it is easy to send the chamber into the sort of continuous discharge that is associated with Geiger counters. The noble gas atoms can become excited or ionized. If they are excited, they can emit a photon when returning to a normal state. This photon will generally have an energy that is higher than the ionization potential of the cathode, so it could cause extraneous electrons to be released from the cathode and produce false avalanches. If the noble gas atoms are ionized, the ions then proceed to the cathode and extract the electron. There is extra energy left over, and another electron is extracted, or a photon is emitted. These processes could lead to a delayed

false avalanche.[1]

To quench extra electrons and avoid spurious avalanches, a gas with polyatomic molecules, often with more than four atoms, is added to the gas mixture. These atoms have a lot of vibrational and rotational energy states, and thus can absorb extra energy and dissipate it through collisions and dissociation. The efficiency of this quenching process generally increases with an increase in the number of atoms in the molecule.[2]

Small amounts of electronegative gas can be added to the mixture to capture free electrons and avoid false avalanches. Such gases include freons or ethyl bromide.[3]

The products of the dissociation, and recombination, of the molecules in the quenching can cause problems. The gas is flowed continuously, so gaseous products will eventually leave the chamber, but some of the products are liquid and solid, and they can deposit inside the chamber, causing field irregularities. Alcohol is bubbled into the gas to inhibit the formation of these deposits.

The ionizations of the avalanche occur about once each time an electron gains enough energy for ionization. A convenient quantity to define is called the first Townsend coefficient, labeled α. This coefficient is equal to the reciprocal of the mean free path between ionizing events, and is therefore the average number of ionization per unit length traversed by an ionizing drift electron.

As the electrons travel a distance dx, αdx ionizations will occur, each liberating an additional electron. Thus the increase in the number of electrons will be

$$dn = n\alpha dx \tag{2.1}$$

integrating the above equation gives

$$n = n_0 e^{\alpha x} \tag{2.2}$$

[1]F. Sauli, *Principles of Operation of Multiwire Proportional and Drift Chambers,* CERN report 77-09, Geneve, Switzerland, 3 May 1977, pp. 46-48

[2]F. Sauli, *Principles of Operation of Multiwire Proportional and Drift Chambers,* CERN report 77-09, Geneve, Switzerland, 3 May 1977, pp. 46-48

[3]F. Sauli, *Principles of Operation of Multiwire Proportional and Drift Chambers,* CERN report 77-09, Geneve, Switzerland, 3 May 1977, pp. 46-48

If n/n_0 is defined as a constant M called the multiplication factor, then[4]

$$M = e^{\alpha x} \tag{2.3}$$

However, for larger gains, it becomes necessary to recognize the E dependence of α (and hence the x dependence of α), thus the multiplication factor becomes

$$M = \exp[\int_{x_1}^{x_2} \alpha(x)dx] \tag{2.4}$$

As the electrons arrive at the anode wires, the positive ions are moving away from the anode. Their velocity depends on the mobility of the ions and the field. So

$$W^+ = \frac{dr}{dt} = \mu^+ E = \mu^+ \frac{C_0 V_0}{2\pi\epsilon_0 r}, \tag{2.5}$$

assuming C_0 is the appropriate capacitance for the detector, V_0 is the relative voltage of the anode, W^+ is the ion drift velocity, μ^+ is the ion mobility, t is time, r is the distance from the center of the anode, and the avalanche occurs very close to the wire where the electric field is proportional to $1/r$. The final asumption is justified because the first Townsend coefficient is only about $4/\text{cm}$ at about $200\mu\text{m}$ from the center of the anode wire when the cathode voltage is set to its highest level in this experiment. The distance of the ions from the center of the anode is, as a function of t,

$$\int_a^r r dr = \frac{r^2 - a^2}{2} = \int_0^t \mu^+ \frac{C_0 V_0}{2\pi\epsilon_0} dt \tag{2.6}$$

$$r(t) = [a^2 + \mu^+ \frac{C_0 V_0}{\pi\epsilon_0} t]^{\frac{1}{2}} = a[1 + \frac{t}{t_0}]^{\frac{1}{2}} \tag{2.7}$$

assuming a is the radius of the anode, and defining t_0, a characteristic time, as:

$$t_0 = \frac{\pi\epsilon_0 a^2}{C_0 V_0 \mu^+} \tag{2.8}$$

[4]F. Sauli, *Principles of Operation of Multiwire Proportional and Drift Chambers,* CERN report 77-09, Geneve, Switzerland, 3 May 1977, p. 37

The potential difference between the drifting electrons and positive ions will be

$$\Delta V = -\frac{Q}{2\pi\epsilon_0 l}\ln\frac{r_+}{r_-} \tag{2.9}$$

Where Q is the charge, r^+ is the distance from the center of the anode to the positive ions, and r^- is the distance from the center of the anode to the electrons. (r^- can be taken to be equal to a.) Combining the above two equations gives the potential difference between the ions and the electrons on the anode wire.

$$V(t) = -\frac{Q}{2\pi\epsilon_0 l}\ln\frac{r(t)}{a} = -\frac{Q}{4\pi\epsilon_0 l}\ln[1+\frac{t}{t_0}] \tag{2.10}$$

The voltage between the anode and cathode is held constant by the high voltage source, so charge flows into the anode wire to compensate for the voltage difference resulting from the outward drifting ions. This charge is given by:

$$q(t) = -C_0 l V(t) \tag{2.11}$$

Where C_0 is the appropriate capacitance per unit length for the chamber geometry, and l is the length. The capacitance per unit length is given by:[5]

$$C_0 = \frac{2\pi\epsilon_0}{\ln(\frac{\pi h}{s}) - \ln(\frac{2\pi a}{s})} \tag{2.12}$$

Where s is the horizontal spacing between wires, and h is the distance between the wire plane and the high voltage cathode plane. Substituting gives,

$$q(t) = -\frac{Q}{2[\ln(\frac{\pi h}{s}) - \ln(\frac{2\pi a}{s})]}\ln[1+\frac{t}{t_0}] \tag{2.13}$$

[5]F. Sauli, *Principles of Operation of Multiwire Proportional and Drift Chambers,* CERN report 77-09, Geneve, Switzerland, 3 May 1977, p. 52.

Differentiating the above with respect to time gives the current for the output signal,[6]

$$I(t) = -\frac{Q}{2t_0[\ln(\frac{\pi h}{s}) - \ln(\frac{2\pi a}{s})]}[\frac{1}{1+\frac{t}{t_0}}] \tag{2.14}$$

This current is of crucial importance. If the maximum current, or current at $t = t_0$, is below a certain thershold level, the pulse will not be detected. This fact is used in chapter 4, section 3.

[6]This equation and many of the steps leading to it are from R. Gilmore, *Single Particle Detection and Measurement,* Taylor and Francis, Washington, DC, 1992, pp. 61-62.

Chapter 3

Construction

3.1 Introduction

The chambers needed to be constructed according to several constraints. The VDCs must have wires which are parallel and evenly placed, and an elaborate procedure was used to insure that this constraint was met. The tension of the wires is also critical and must be well regulated. The cathode planes had to be very flat with uniform spacing, so the electric field follows the same pattern everywhere. Also, the chamber has to be air tight to preserve the purity of the gas inside, and it must be strong enough to handle its own weight.

The chambers were constructed by placing anode wires in a frame, making gold plated mylar high voltage windows for the cathode planes, and making gas containment windows from aluminum mylar. The frames and windows were then placed in a larger gas containment box.

3.2 Wire placement and tension

The anode wires were made of tungsten and coated with gold, and 20 μm in diameter. An elaborate procedure was used to insure that the wires are spaced uniformly and the tension on them is correct. The spacing is critical because the location of each wire needs to be known to find the position as in figure 2-1. The tension must be great

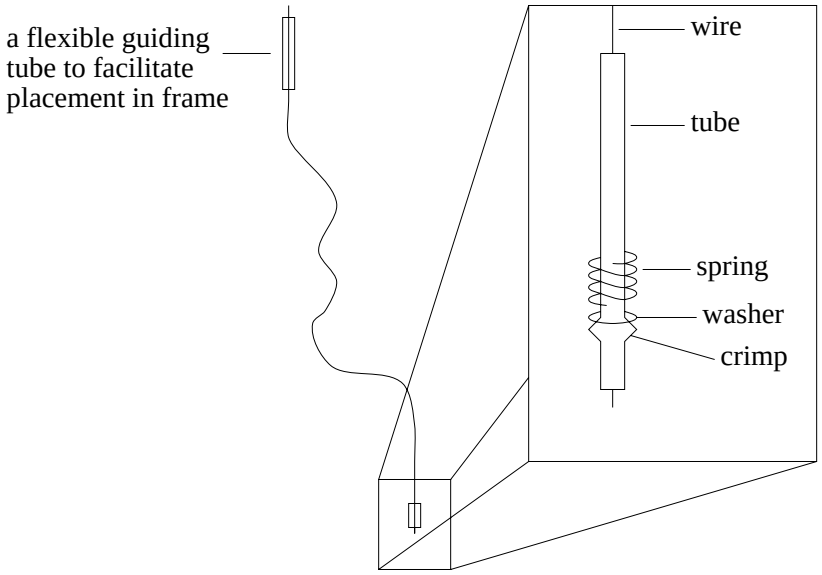

Figure 3-1: A Prepared Wire

enough to keep the wires in the same plane. If the wires are not sufficiently taunt, they could find an alternate equilibrium in which the wires are alternately spaced up and down, instead of being straight and in the same plane. The tension in the wires in these VDCs is .686 Newtons.

To prepare the wires for placement in the chamber, they were inserted in a small tube with a hole with a diameter of 100 μm. The tube was then crimped, thus holding the wire in place. A washer and a spring were added to the wire. The wire was threaded through the washer, so the washer fell far enough along the wire to reach the tube, and the place where the tube was crimped. The wire is then threaded through a spring, which is held in place by the washer. The wire thus prepared is shown schematically in figure 3-1. A flexible guiding tube was added to the wire to help install the washer and spring, and to eventually help guide the wire when placing it in the frame.

The wire is then threaded into a mounting tube glued to the frame. There is a mounting tube on one side of the frame into which the wire is initially inserted, and another mounting tube on the other side where the other end of the wire must be placed. After the wire is threaded through the second side, it is threaded through another of the small tubes with a 100μ hole, onto which a washer has previously been

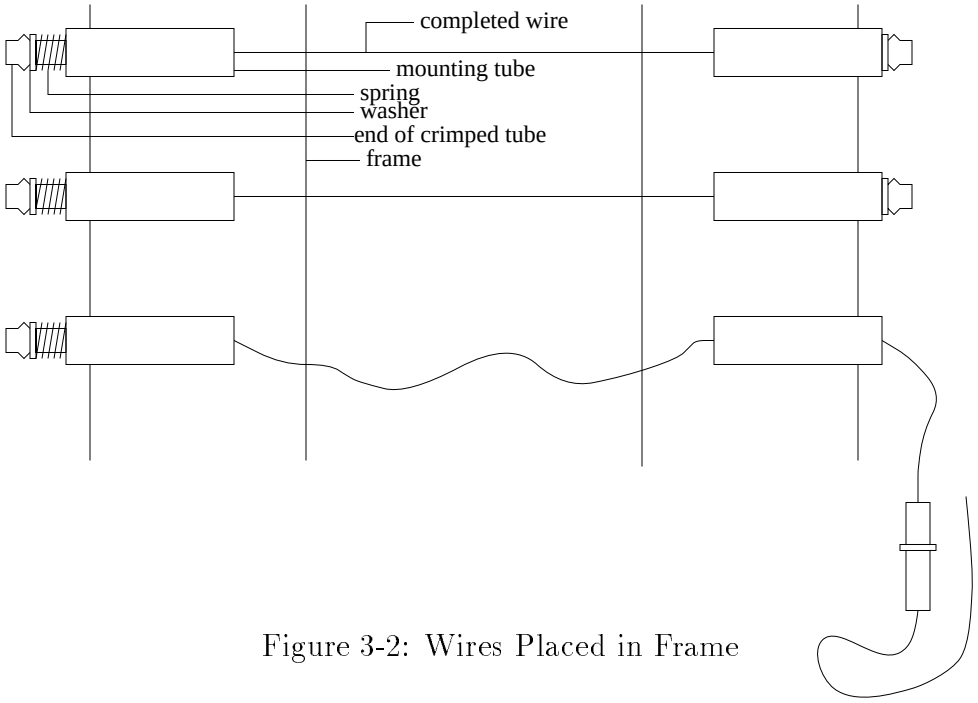

Figure 3-2: Wires Placed in Frame

threaded. At this point the wire is represented by the incompletely strung slack wire in figure 3-2.

The small tube is then placed inside the larger mounting tube attached to the frame. A block is used on the other side of the frame to push the crimped tube on that end of the wire inward by a constant length for every wire, slightly compressing the spring. At this point, a weight is attached to the end of the wire, so the wires have a constant regulated tension. (see figures 3-3, and 3-4)

The wire is then crimped inside the smaller tube, with the weight and pulley system holding it in place with the constant tension. The excess wire is then cut away, as in figure 3-4, and the block is removed from the other side of the frame. If the end with the spring which was compressed by the block moved too far after the block was removed, the wire was improperly crimped and had to be rejected and replaced with another wire. This process had to be repeated hundreds of times for each frame, once for each wire. There are two of these wire frames in each chamber. The wires in a single frame are parallel to one another and at an angle of 45 degrees to the edge of

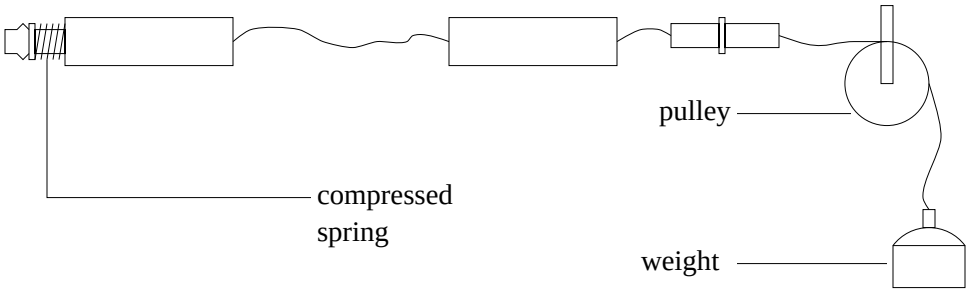

Figure 3-3: Weight Is Being Attached to Wire

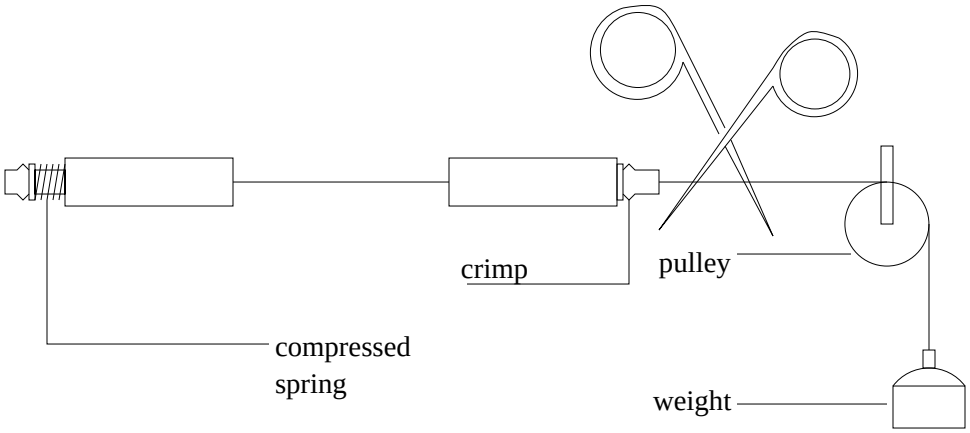

Figure 3-4: Wire Is Cut

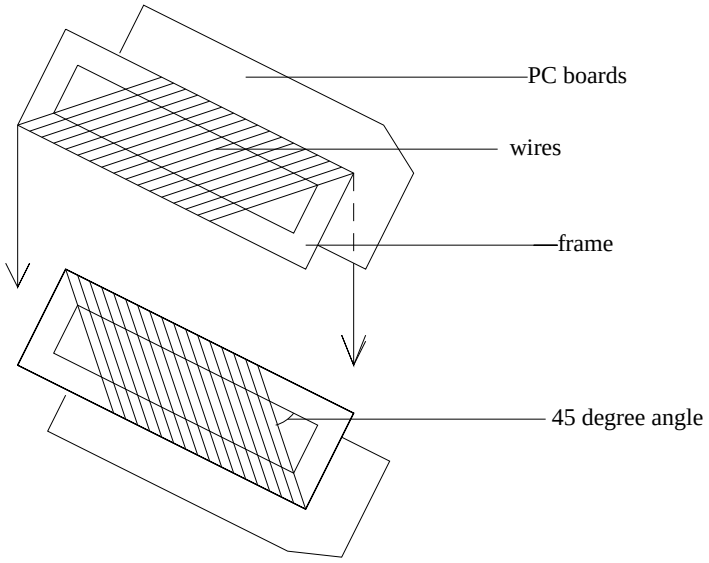

Figure 3-5: Orientation of Wires and Frames

the frame itself. (figure 3-2 was drawn with the wires perpendicular to the edge of the frame for simplicity, the angles in figure 3-5 are more accurate) The wires in the two frames were offset by 90 degrees, in other words, compared to the edge of the chamber, one frame had wires which made an angle of 45 degrees with the chamber's edge, while the wires in the other frame made an angle of 135 degrees with the chamber's edge if one is using a common reference. See figure 3-5.

The wire frames included printed circuit (PC) boards, and small jumpers were used to make the connections between the circuit boards and one end of each wire, the end without the spring. The PC boards included conductive strips which made an electrical connection with the anode wires and connectors for the amplifier cards, which were further away from the frame itself. See figure 3-6. The amplifier/discriminator cards amplify the signals from the wires. If the amplified signal is large enough to overcome a set threshold level, then a logic pulse is emitted. The logic pulse is delayed by a constant time for each wire, so relative timing accuracy is maintained.

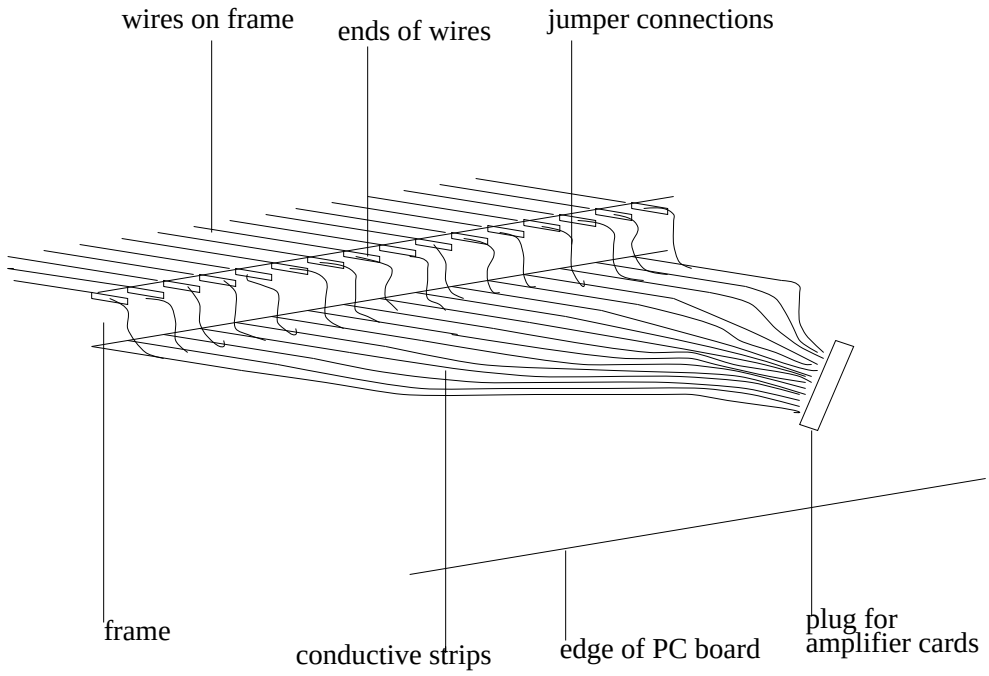

Figure 3-6: Wires Connected to Printed Circuit Boards

3.3 Gas and high voltage cathode planes, and overall assembly

The gas and high voltage planes were constructed as follows. A sheet of metallized mylar foil, 0.00025 inches thick, was placed in a special stretching frame which allowed the mylar foil to be stretched until it was taunt and smooth. The frame which holds this foil (the "window frame") was coated with a special glue (designed, like all VDC components, to minimize gas leakage) and placed on a table face up. The mylar (still on the stretcher frame) was placed on top of the glue-coated surface of the window frame. A spare window frame was placed on top of this assembly, and weights were distributed along this spare frame, ensuring that the mylar was firmly pressed against the glue. The entire assembly was left this way for about 24 hours to allow the glue to completely dry. Afterwards the excess mylar could be cut away from the chamber frame, leaving only the mylar that is stuck to the frame with the glue, and the mylar which is inside the frame. See figure 3-7.

The planes and wire frames were then assembled, with the wire frames surrounding

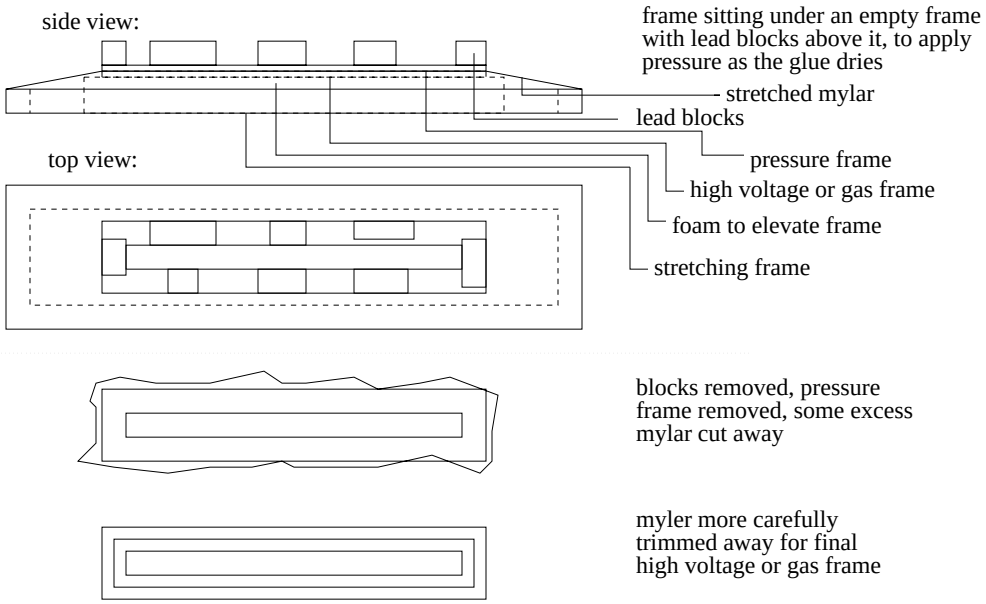

Figure 3-7: High Voltage and Gas Plane Preparation

the middle high voltage plane, which is a mylar plane with both sides coated with gold. Two outer mylar high voltage planes, with only the inner side coated with gold, surrounded the wire frames. The aluminized-mylar gas-containment windows are on the outside of the wires and high voltage planes. The whole assembly is positioned in a larger gas containment frame. See figure 3-8. The PC boards extend outward so the electrical connections to the anode wires are accessible, and there are inlets and outlets on the large gas containment box for the high voltage connection to the cathode planes and the gas. The frames include holes which are placed on alternating ends of the various individual frames. This placement forces gas to flow through all sections of the chamber.

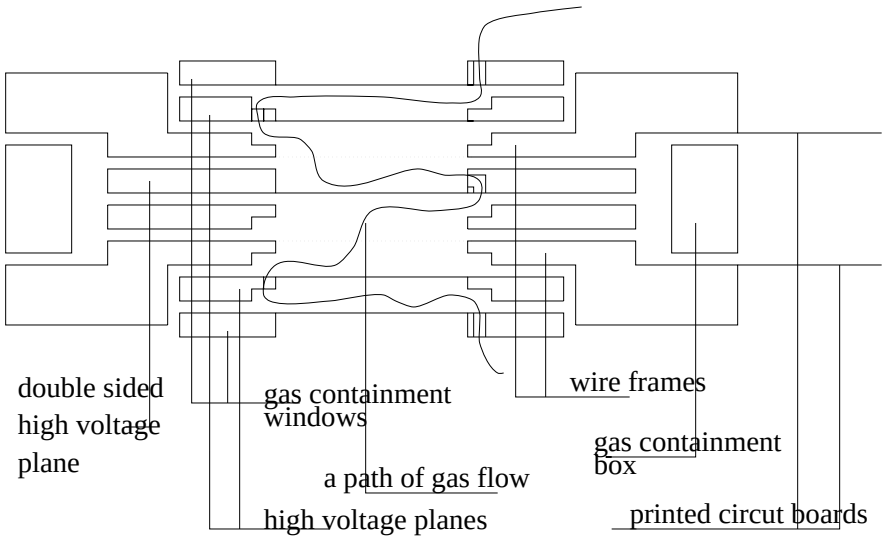

Figure 3-8: A Cross Section of Complete Chamber

Chapter 4

Experiment

4.1 Setup

The measurements performed here involved using two VDC packages of crossed wires, one on top of the other, as they will be used permanently. Scintillation detectors were placed above and below the chambers, as in figure 4-1. The scintillation detectors were optically connected to two photomultiplier tubes. The scintillation detector gives off a flash of light as a particle passes through it, and the photomultiplier tubes then convert it into an electrical pulse. There were two photomultplier tubes attached to each of the two scintillation detectors, to make four in all. In order for the electronics to be triggered, a certain number of the photomultplier tubes had to give a pulse. The number was either three or four, with some data files taken with each setting. For all data files, the gas flowing through the chamber was 38% ethane, 62% argon.

The scintillator signal was used as both a trigger and a common stop. After the signal was used as a trigger, it was sent through a delay cable. This delayed signal marked the end time point for a set of time-to-digital converters (TDCs). If accurate measurement of drift times are required, it is necessary to record the times at which the individual photomultplier tubes gave signals, but such measures are not necessary for the measurement of efficiency.

The TDCs change the time difference between a pair of signals into a number that is proportional to the time difference. The time difference here is the difference between

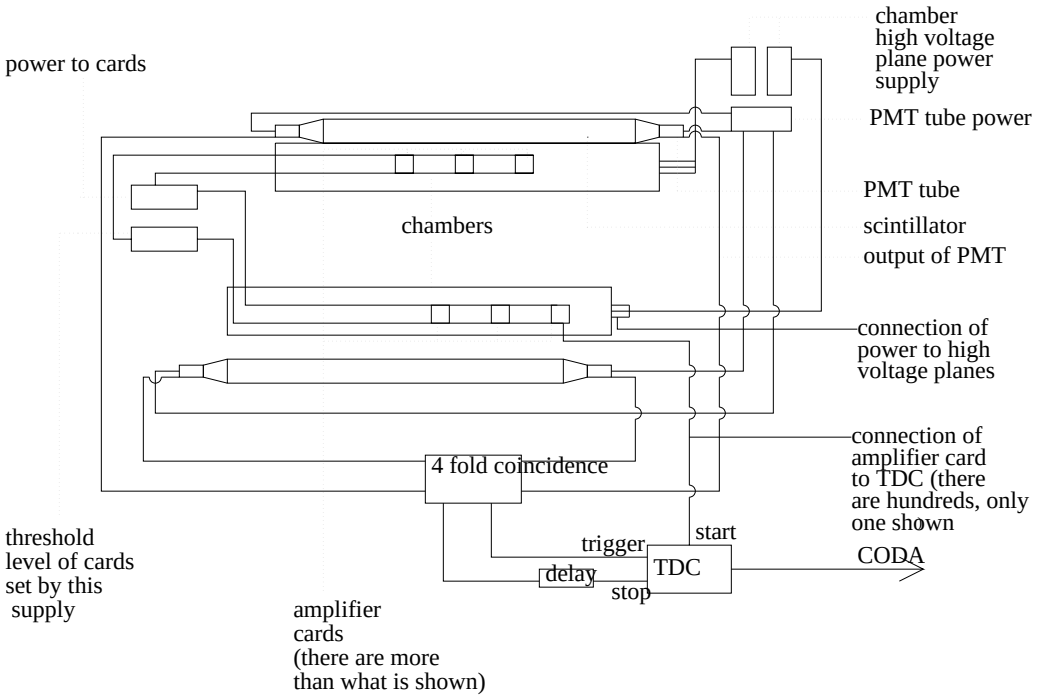

Figure 4-1: Experimental Setup

the time of the wire pulse and the time of the common stop from the scintillator signal. The wires were connected to the TDCs with flat ECL cables. The fact that the signal was delayed and used as a stop means that the longer times in the TDC signify earlier pulses from the wires. These times were then given via a data acquisition system to an analysis program.

4.2 Efficiency Calculation

The program also recorded which wires gave pulses in a given event. It had an algorithm to discover when a wire was supposed to fire but did not, indicating an inefficiency. It examined situations in which two wires fired, and there was an additional wire between them. If the wire in between fired, it was counted as a time in which the wire behaved efficiently, and when the wire in between did not fire, it was counted as a time the wire behaved inefficiently. The efficiency is then the number of times the wire was efficient divided by the sum of the times the wire was inefficient

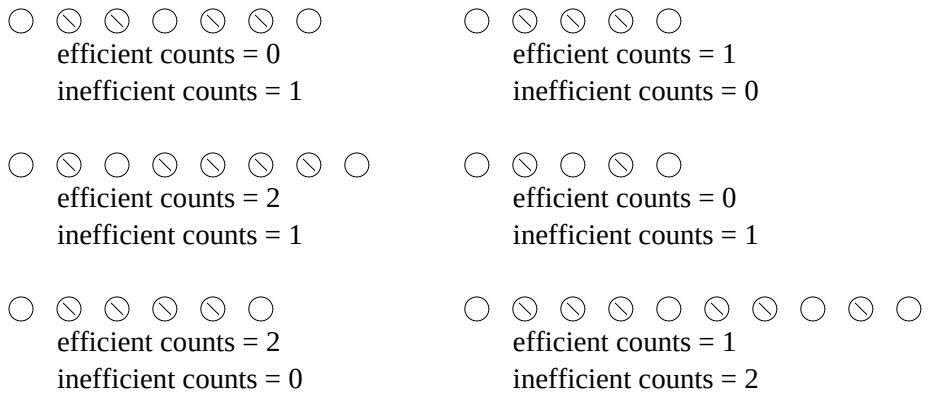

Figure 4-2: Efficiency Algorithm - Sets of wires are shown as rows of circles. Empty circles represent wires that give no pulse, and circles with lines in them represent wires which give a pulse. The results of the algorithm are given below the row of circles.

and the number of times it was efficient. Figure 4-2 illustrates several sets of wires and what the algorithm would output for each situation.

A global efficiency for the entire chamber can be found by adding all of the efficient counts for all wires, and dividing the sum by the total of all the counts on all wires both efficient and inefficient. If κ represents the total number of times any wire in the chamber was efficient for the duration of a data taking run, and ϑ represents the number of times that any wire in the chamber is found to be inefficient during the data run, then

$$\epsilon = \frac{\kappa}{\kappa + \vartheta} \tag{4.1}$$

Where ϵ is the total chamber efficiency. For cases in which the efficiency is high, the uncertainty can be intuitively seen by approximating the occurance of inefficient counts as a poisson process. This would make the uncertainty in the efficiency

$$\sigma_\epsilon = \frac{\sqrt{\vartheta}}{\kappa + \vartheta} \tag{4.2}$$

However, when the efficiency is too low, the binomial treatment must be used. For

a binomial distribution, when p is the probability of success in a trial, and n is the number of trials, then the uncertainty in the number of successes is given by:[1]

$$\sqrt{np(1-p)} \tag{4.3}$$

In this case, $n = \kappa + \vartheta$, and $p = \frac{\kappa}{\kappa+\vartheta}$, so

$$\text{sucesses} = \sqrt{(\kappa+\vartheta)\frac{\kappa}{\kappa+\vartheta}(1-\frac{\kappa}{\kappa+\vartheta})} \tag{4.4}$$

simplifying the above yields,

$$\sqrt{\kappa(1-\frac{\kappa}{\kappa+\vartheta})} \tag{4.5}$$

The result is not the uncertainty in the efficiency itself, but rather the uncertainty in the number of successes, or efficient counts. This must be divided by the total number of counts to obtain the uncertainty in the efficiency. Thus,

$$\sigma_{Eff} = \frac{\sqrt{\kappa(1-\frac{\kappa}{\kappa+\vartheta})}}{\kappa+\vartheta} \tag{4.6}$$

also,

$$\sigma_{Eff} = \frac{\sqrt{\kappa(\frac{\kappa+\vartheta}{\kappa+\vartheta}-\frac{\kappa}{\kappa+\vartheta})}}{\kappa+\vartheta} = \frac{\sqrt{\kappa(\frac{\vartheta}{\kappa+\vartheta})}}{\kappa+\vartheta} = \frac{\sqrt{\vartheta(\frac{\kappa}{\kappa+\vartheta})}}{\kappa+\vartheta} \tag{4.7}$$

Taking the limit of a piece of the numerator in the last expression gives:

$$\lim_{\frac{\vartheta}{\kappa}\to 0} \frac{\kappa}{\kappa+\vartheta} = 1 \tag{4.8}$$

Substituting gives,

$$\lim_{\frac{\vartheta}{\kappa}\to 0} \frac{\sqrt{\vartheta(\frac{\kappa}{\kappa+\vartheta})}}{\kappa+\vartheta} = \frac{\sqrt{\vartheta}}{\kappa+\vartheta} \tag{4.9}$$

Which is the same as the uncertainty in the efficiency found for high values of efficiency when inefficient counts are assumed to be a poisson process.

[1] R. Bevington, *Data Reduction and Error Analysis for the Physical Sciences,* McGraw-Hill, New York, NY, 1992, p. 20.

Some of the experimental results were put into the form of graphs giving the efficiency as a function of high voltage, with the threshold held constant, and the scintillators in the same position. Other graphs include data taken with the same threshold voltage, and different high voltage settings, with the scintillator position fixed as before. Generally, an efficiency plateau of 99% was reached when the threshold voltage on the cards was set to 3.0 V and the high voltage on the planes was 4.1 kV or greater. The plateau was reached at 4.0 kV or greater on the high voltage planes when the threshold level was set to 2.5 V. However, there are some lower efficiency measurements with those conditions. This was likely due to changes in the scintillator positions, as explained in appendix B.

The graphs are as follows:

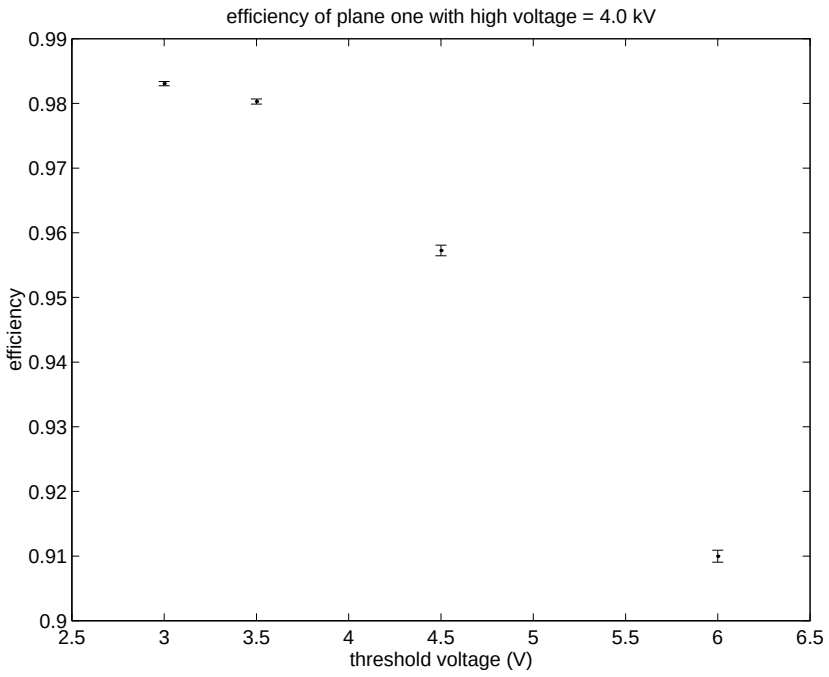

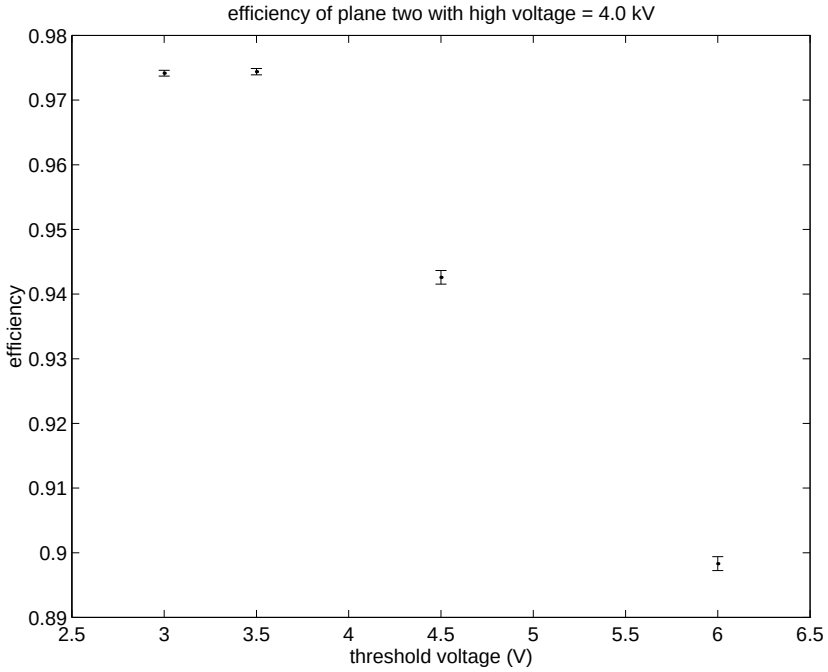
efficiency of plane two with high voltage = 4.0 kV
efficiency
threshold voltage (V)
0.98
0.97
0.96
0.95
0.94
0.93
0.92
0.91
0.9
0.89
2.5
3
3.5
4
4.5
5
5.5
6
6.5

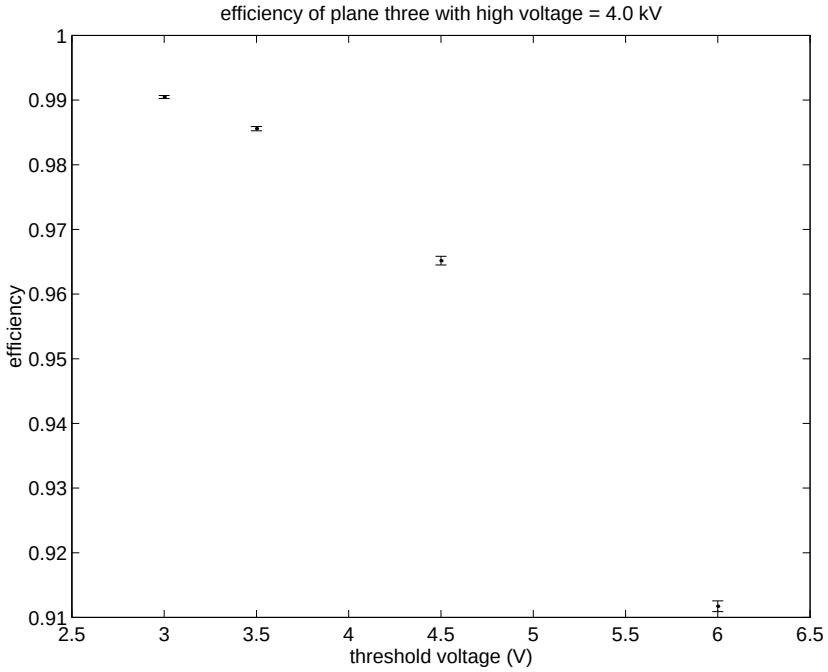
efficiency of plane three with high voltage = 4.0 kV
efficiency
threshold voltage (V)
1
0.99
0.98
0.97
0.96
0.95
0.94
0.93
0.92
0.91
2.5
3
3.5
4
4.5
5
5.5
6
6.5

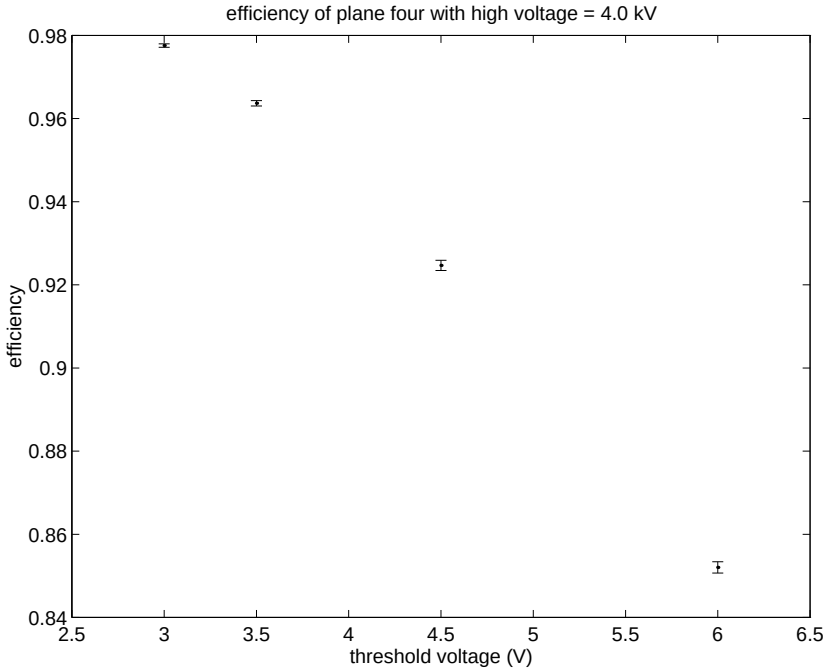
efficiency of plane four with high voltage = 4.0 kV
efficiency
threshold voltage (V)
0.98
0.96
0.94
0.92
0.9
0.88
0.86
0.84
2.5
3
3.5
4
4.5
5
5.5
6
6.5

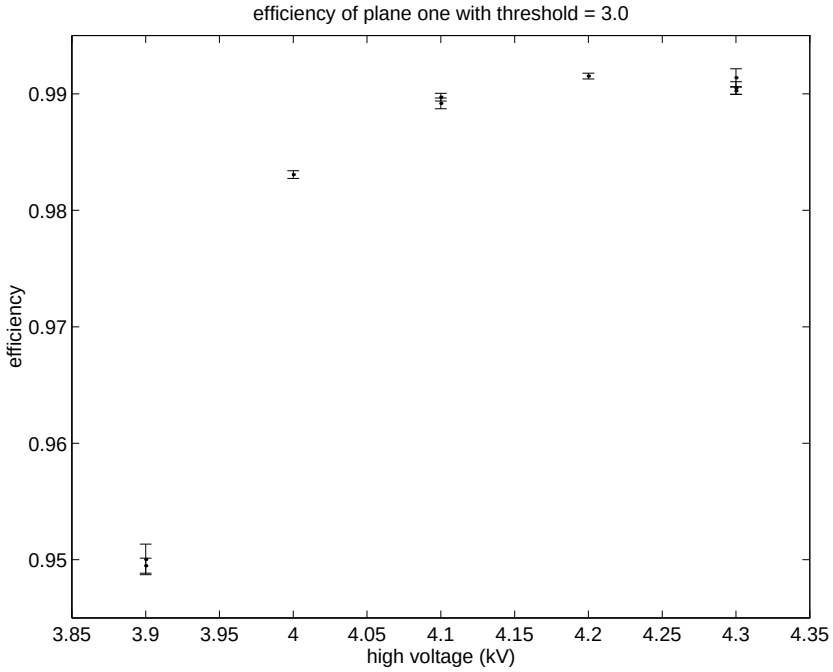
efficiency of plane one with threshold = 3.0
efficiency
high voltage (kV)
0.99
0.98
0.97
0.96
0.95
3.85
3.9
3.95
4
4.05
4.1
4.15
4.2
4.25
4.3
4.35

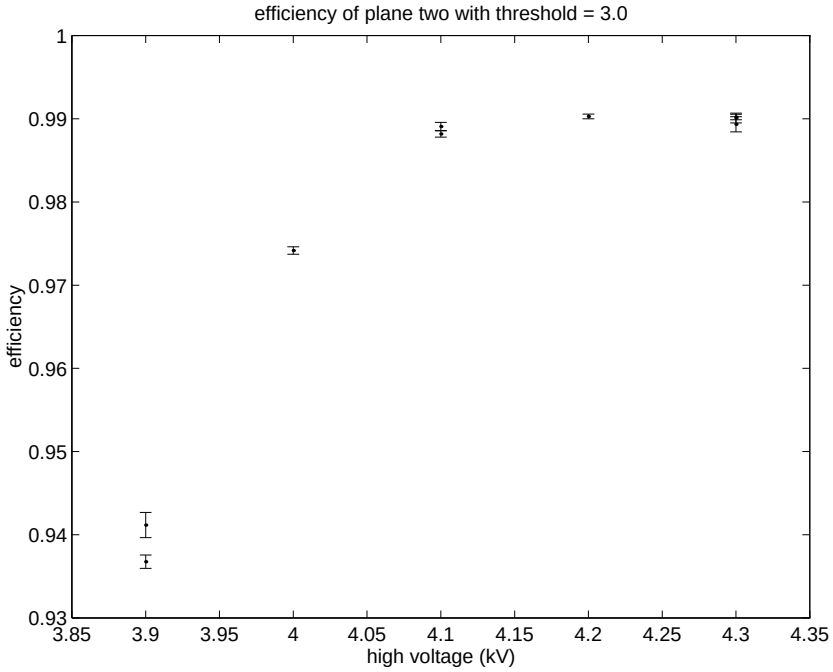
efficiency of plane two with threshold = 3.0
efficiency
high voltage (kV)
1
0.99
0.98
0.97
0.96
0.95
0.94
0.93
3.85
3.9
3.95
4
4.05
4.1
4.15
4.2
4.25
4.3
4.35

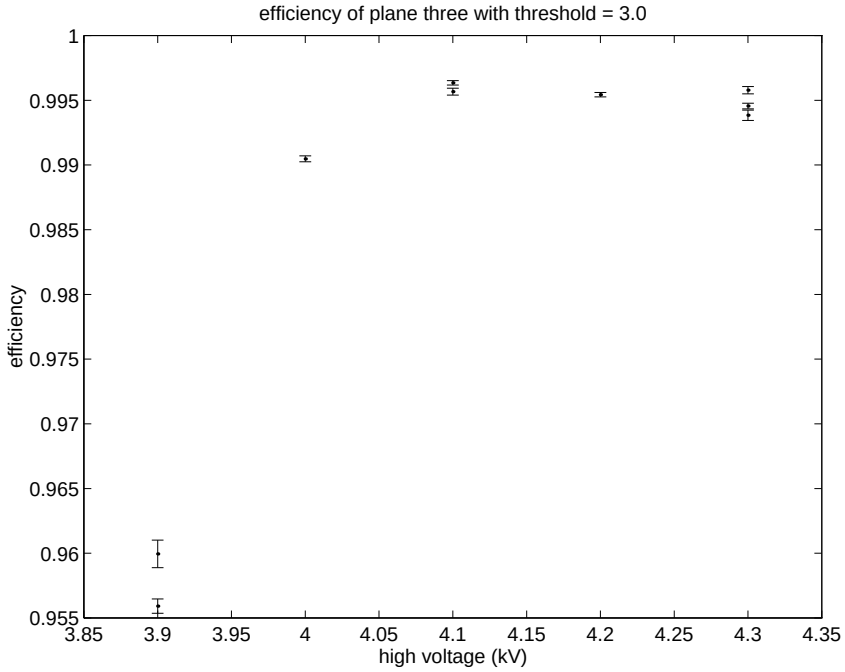
efficiency of plane three with threshold = 3.0
efficiency
high voltage (kV)
1
0.995
0.99
0.985
0.98
0.975
0.97
0.965
0.96
0.955
3.85
3.9
3.95
4
4.05
4.1
4.15
4.2
4.25
4.3
4.35

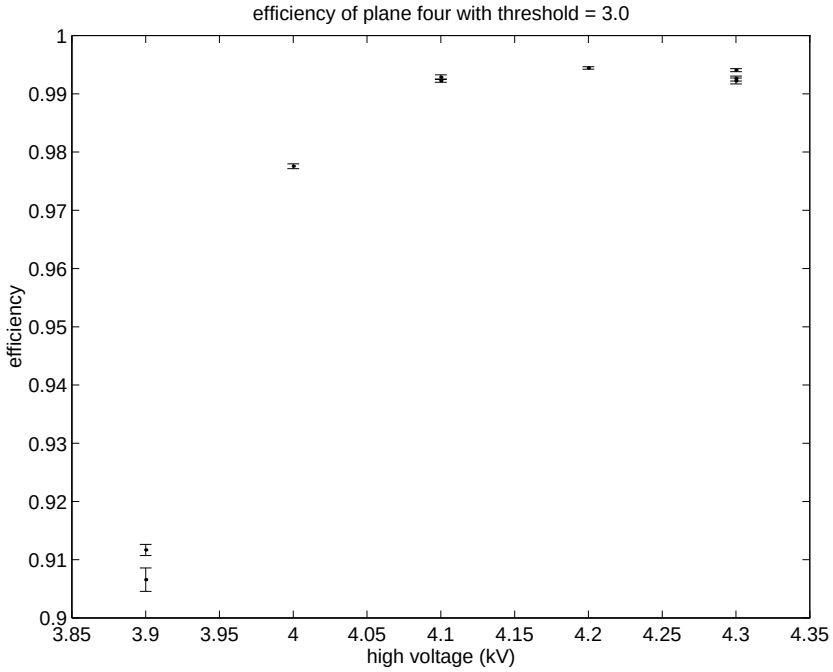

4.3 The Multiplication Factor

Given a model for the avalanche process, the measured efficiency values can be used to deduce the current that was carried in the average wire pulse. From this current an estimate of the multiplication factor can be found, after manipulating equation 2.14 into giving Q as a function of I. This multiplication factor can then be compared to the multiplication factor found from equation 2.4. However there are factors which cause discrepancies between the two.

According to Garfield, a chamber analysis program, the Townsend coefficient α for the gas mixture used in this experiment (62% argon 38% ethane) is given as a function of electric field by the following table (For lower values of the field, α is zero because the electrons do not gain enough energy between collisions to cause ionizations.):[2]

[2]Computer Program GARFIELD, R. Veenhof, http://consult.cern.ch/writenp/garfield/main.html

E-field (V/cm)	α (1/cm)
10019	.0794922
14412	4.15596
20731	38.7971
29821	164.907
42896	450.869
61703	948.868
88757	1679.15
127670	2678.98
183650	3929.58
264170	5442.38
380000	7235.49

To give an idea of the distances involved: For a high voltage setting of 4300 V, the distance from the center of the anode where the field is 10019 V/cm is 2954 μm. For the same voltage setting, the distance from the center of the anode where the field is 61703 V is 480 μm. For a lower setting of 3500 V, the distance corresponding to 10019 V/cm is 1672 μm, and the distance corresponding to 61703 V is 390 μm. These distances were calculated using equation 4.11 below.

The Garfield analysis program gave the value for the electric field at the radius of the wire as being near 296000 V/cm.[3] Noting the fact that E is inversely proportional to the distance from the center of the wire then gives:

$$E = (296000V/cm)\frac{.001cm}{r} \tag{4.10}$$

Where r is the distance from the center of the anode wire in cm, and .001 cm is the

[3]Computer Program GARFIELD, R. Veenhof, http://consult.cern.ch/writenp/garfield/main.html

anode wire radius. Using this equation, one can find $r(E)$:

$$r = \frac{296V}{E} \tag{4.11}$$

where the electric field E is in V/cm. Therefore, one can find the r values which correspond to the various E field values found in the above table, and thus approximate α as a function of r. This approximate expression can then be used in the integral in equation 2.4. With the completion of this integral, the multiplication factor can be calculated. Using the data above, and assuming that the electric field at the radius of the anode wire is proportional to the high voltage applied to the cathode planes, similar calculations can be performed for each chamber voltage. Results of those calculations are as follows:

high voltage	integral	Mult. factor
4300	12.375	2.369e5
4200	11.948	1.544e5
4100	11.523	1.010e5
4000	11.102	6.629e4
3900	10.684	4.365e4
3700	9.843	1.883e4
3500	9.030	8.347e3

The next method of finding the multiplication factor uses the efficiency data. It involves the distribution of pulse heights, for the current in the pulses from the anode wires. When an expression for the probability distribution for the pulse height of the current is found, it can be integrated from zero to the minimum height required to trigger the threshold voltage of the card. This current height can be converted into the units of threshold voltage by noting that a current of 2μA is needed to overcome a threshold voltage of one volt applied to the cards, and the currents needed to overcome

other voltages are proportional to the threshold voltage. The pulse height, or maximum current in an individual pulse, is the current of intrest because that is the value which must be large enough overcome the threshold. The pulse height is the current when $t = 0$ in equation 2.14.

The multiplication is given by the Furry Distribution, which can be approximated in the limit of large M by:[4]

$$P(m) = \frac{1}{M} \exp\left(\frac{-m}{M}\right) \tag{4.12}$$

where $P(m)$ is the probability of a given avalanche yielding m electrons from a single primary electron, M is the mean number of electrons resulting from one primary electron, in other words M is the multiplication factor. The equation can be integrated to yield the probability that a given avalanche will not multiply beyond a certain critical number of electrons, m_c.

$$P(m < m_c) = \int_0^{m_c} \frac{1}{M} \exp\left(\frac{-m}{M}\right) dm = \exp\left(\frac{-m}{M}\right)\Big|_{m_c}^{0} = 1 - \exp\frac{-m_c}{M} \tag{4.13}$$

thus,

$$\frac{-m_c}{M} = \ln(1 - P(M < M_c)) \tag{4.14}$$

The efficiency is simply $1 - P(M < M_c)$, so

$$\frac{-m_c}{M} = \ln \epsilon \tag{4.15}$$

where ϵ is the efficiency. Rearranging yields

$$M = \frac{-m_c}{\ln \epsilon} \tag{4.16}$$

The efficiency has been measured, and m_c can be found from the threshold voltage with the aid of a few more equations.

[4]R. Gilmore, *Single Particle Detection and Measurement,* Taylor and Francis, Washington, DC, 1992, p. 64.

Rearranging 2.14 to yield charge as a function of current, the charge corresponding to the current pulse which is the minimum needed to overcome the threshold can be found, given the minimum necessary current pulse. The height of this minimum current pulse can be found from the threshold voltage setting and the conversion:

$$I = V_{th}(2\mu A/V) \tag{4.17}$$

Rearranging 2.14 yields,

$$Q = I2t_0[\ln(\frac{\pi h}{s}) - \ln(\frac{2\pi a}{s})][1 + \frac{t}{t_0}] \tag{4.18}$$

Dividing the charge from the last equation by the factor $1.6022e - 19Coul/e^-$ will yield m_c. Thus the quantities on the right side of equation 4.16 are known, and the multplication factor can be found.

The above calculations can be done to find a multiplication factor for each high voltage setting. The data was searched in order to find the most efficient planes with each of the seven high voltage settings represented in the data files. The results are in the following table, with ϵ representing the efficiency, I_c representing the minimum current pulse height necessary to overcome the thershold (in Amperes), m_c representing the minimum number of electrons needed in the avalanche for the pulse to reach I_c. The resultant number of electrons in the entire avalance is represented by M'.

$hv(V)$	V_{th}	ϵ	I_c	m_c	M'
3500	2.5	.609	5e-6	2.741e5	5.526e5
3700	2.5	.75	5e-5	2.593e5	9.012e5
3900	2.5	.97663	5e-6	2.460e5	1.040e7
4000	2.5	.99434	5e-6	2.398e5	4.225e7
4100	3.0	.99635	6e-6	2.808e5	7.668e7
4200	2.5	.99636	5e-6	2.284e5	6.263e7
4300	3.0	.99578	6e-6	2.677e5	6.330e7

When using equation 4.18, the mobility is needed in the equation for t_0. The program Garfield gave the mobility for argon ions in a gas of 50% argon and 50% ethane to be 1.8 $cm^2/(Vsec)$. The program also gave the mobility for a gas of 80% argon and 20% ethane as 1.9 $cm^2/(Vsec)$.[5] The value used in the equation was 1.85 because the gas mixture used in the experiment is 62% argon and 38% ethane. The capacitance per unit length is also needed to find t_0, and to find this capacitance using equation 2.12, the distance between the cathode and anode (h) is needed, as well as the horizontal wire spacing (s), and the anode radius (a). The anode radius is .001cm, the anode-cathode distance is 13mm, and the interwire spacing is 4.24mm.

The picture above is oversimplified, since it assumes that only one primary electron is responsible for the detected signal. However, the electrons from more than one ionization event contribute to the total avalanche signal. The Garfield chamber simulation program predicts an average of 31 primary electrons per cm of distance covered by the particle.[6] The path length of an incident particle over a single drift cell (a drift cell being defined as the volume in which all electrons drift towards the same wire) can be calculated as follows: The sense wires are 4.24mm apart, and they make an angle of 45 degrees with the lengthwise edge of the chamber, so if the particles cross the chamber at roughly 45 degree angles, there will be about 31 times .424 times two factors of $\sqrt{2}$, or about 26 ionization events per track in each drift cell. Furthermore, each primary ionization event can result in a cluster of several drift electrons being liberated, if the energy transfer in the collision is large enough. The number of electrons in this cluster is given by a probability distribution with a mean of about 2.4.[7] Convolving these distributions (clusters per drift cell and electrons per cluster) will result in an average of roughly 42 electrons per track per drift cell, which are available for creating avalanches.

It is not, however, correct to simply assume that we must multiply all the signal

[5]Computer Program GARFIELD, R. Veenhof, http://consult.cern.ch/writenp/garfield/main.html

[6]Computer Program GARFIELD, R. Veenhof, http://consult.cern.ch/writenp/garfield/main.html

[7]Computer Program GARFIELD, R. Veenhof, http://consult.cern.ch/writenp/garfield/main.html

sizes by 42 in order to account for this phenomenon. First, it is important to remember that this factor of 42 is the mean of a complex distribution. Also, these various drifting electrons will not all reach the anode wire at the same time, since they are created in various regions in the drift cell. If electrons from any two clusters form avalanches which reach the anode wire with enough of a time difference, the detection electronics will not see these current bursts as a large single current pulse; it will see two smaller current bursts, and the threshold may not be overcome whereas it would be if the pulses were closer together in time.

There is another effect of possible importance in the efficiency calculations. For large enough gains (10^4–10^5 and above, dependent on the details of the chamber geometry and ion mobilities), the electric field near the wire may be altered by the presence of large numbers of positive ions near the wire after an avalanche. If this effect is present, the multplication factor for later avalanches (for a given track thru the cell) will be lower than for the earlier avalanches. This phenomenon is very complex and is beyond the scope of this thesis; even the Garfield program does not account for this effect in its simulations.

Each of the above effects have some degree of influence on making correct computations of the quantities in the above table. Thus the results presented there, which are not corrected for these effects, should be regarded with proper caution.

Appendix A

Tabulation of Results

Below is a tabulation of results, and a description of data file irregularities. The first column is the data file number, indicating the sequence in which the files were taken. The next entry is the high voltage setting under which that data file was taken (HV in kV), and the next entry is the threshold voltage to the amplifier cards (Th in V). The next number is the wire plane. The entries in the fifth and sixth colums are the total number of inefficient counts (ϑ) and efficient counts (κ), respectively. The next column includes the efficiency measured (ϵ) and the final column is the uncertainty in the efficiency (σ_ϵ) given by equation 4.6.

file	HV(kV)	Th (V)	plane	ϑ	κ	ϵ	σ_ϵ
14	4.1	2.5	1	208	24919	.99172	.00057
			2	218	19858	.98914	.00073
			3	102	26348	.99614	.00038
			4	129	17775	.99280	.00063
15	3.5	2.5	1	847	764	.474	.012
			2	527	651	.553	.014
			3	583	620	.515	.014
			4	273	425	.609	.018
16	3.7	2.5	1	5070	15206	.7500	.0030
			2	3725	10671	.7412	.0037
			3	5100	10695	.6771	.0037
			4	2777	4893	.6379	.0055
17	3.9	2.5	1	593	32783	.98223	.00072
			2	620	25599	.97635	.00094
			3	776	32429	.97663	.00083
			4	1125	19366	.9451	.0016
18	4.0	2.5	1	256	30221	.99160	.00052
			2	264	24400	.98930	.00066
			3	178	31266	.99434	.00042
			4	282	20381	.98635	.00081
19	4.0	3.5	1	609	30310	.98030	.00079
			2	656	24968	.97440	.00099
			3	464	31728	.98559	.00066
			4	746	19795	.9637	.0013
20	4.1	3.0	1	138	12619	.98918	.00092
			2	118	10674	.9891	.0010
			3	66	15176	.99567	.00053
			4	79	10976	.99285	.00080

21	4.0	3.0	1	635	36864	.98307	.00067
			2	813	30660	.97417	.00089
			3	432	44922	.99047	.00046
			4	712	31025	.97757	.00083
22	4.1	3.0	1	243	23378	.98971	.00066
			2	239	19963	.98817	.00076
			3	114	31089	.99635	.00034
			4	178	22852	.99227	.00058
23	3.9	3.0	1	1456	27368	.9495	.0013
			2	1453	21522	.9368	.0016
			3	1531	33198	.9559	.0011
			4	1917	19788	.9117	.0019
24	3.9	3.0	1	345	6559	.9500	.0026
			2	354	5663	.9412	.0030
			3	341	8174	.9600	.0021
			4	490	4755	.9066	.0040
25	4.3	3.0	1	239	24304	.99026	.00063
			2	213	21538	.99021	.00067
			3	154	28147	.99456	.00044
			4	132	22081	.99406	.00052
26	4.3	3.0	1	31	3564	.9914	.0015
			2	34	3154	.9893	.0018
			3	57	13448	.99578	.00056
			4	75	10085	.99262	.00085
27	4.0	4.5	1	308	4734	.9389	.0034
			2	218	3932	.9475	.0035
			3	258	5828	.9576	.0026
			4	309	3559	.9201	.0044

28	4.0	4.5	1	646	14468	.9573	.0016
			2	694	11395	.9426	.0021
			3	637	17652	.9652	.0014
			4	871	10693	.9247	.0025
29	4.3	3.0	1	77	8024	.9905	.0011
			2	71	7093	.9901	.0012
			3	58	9361	.99384	.00081
			4	58	7389	.9922	.0010
30	4.2	2.5	1	49	5747	.9915	.0012
			2	47	5052	.9908	.0013
			3	25	6834	.99636	.00073
			4	21	5086	.99589	.00090
31	4.2	2.5	1	281	34200	.99185	.00048
			2	261	29942	.99136	.00053
			3	166	40750	.99594	.00031
			4	155	30270	.99491	.00041
32	4.2	3.0	1	294	34380	.99152	.00049
			2	291	29648	.99028	.00057
			3	186	40545	.99543	.00033
			4	171	30590	.99444	.00042
33	4.0	6.0	1	2175	21986	.9100	.0018
			2	1992	17598	.8983	.0022
			3	2543	26264	.9117	.0017
			4	2496	14373	.8520	.0027

35	4.1	4.5	1	436	33843	.98728	.00061
			2	450	28977	.98471	.00072
			3	223	40840	.99457	.00036
			4	427	28958	.98547	.00070
36	4.1	4.5	1	113	7945	.9860	.0013
			2	136	6516	.9796	.0017
			3	62	9260	.99335	.00084
			4	120	6356	.9815	.0017
37	4.1	6.0	1	750	26727	.97270	.00098
			2	800	22074	.9650	.0012
			3	644	32696	.98068	.00075
			4	963	21342	.9568	.0014
38	4.1	2.5	1	475	23268	.97999	.00091
			2	420	21855	.98114	.00091
			3	173	20678	.99170	.00063
			4	161	19941	.99199	.00063
39	4.1	3.5	1	531	26962	.98069	.00083
			2	500	24940	.98035	.00087
			3	227	23667	.99050	.00063
			4	195	22919	.99156	.00060
40	4.1	4.5	1	306	13233	.9774	.0013
			2	277	12214	.9778	.0013
			3	105	11570	.99101	.00087
			4	118	11117	.98950	.00096

41	4.1	3.0	1	193	10746	.9824	.0013
			2	181	10152	.9825	.0013
			3	84	9310	.99106	.00097
			4	87	9410	.99084	.00098
42	4.1	3.0	1	856	44357	.98107	.00064
			2	728	41047	.98257	.00064
			3	374	38663	.99042	.00049
			4	324	37251	.99138	.00048
43	4.1	3.0	1	234	10702	.9786	.0014
			2	182	10244	.9825	.0013
			3	84	8995	.9907	.0010
			4	82	9138	.99111	.00098
44	4.2	3.0	1	835	41155	.98011	.00068
			2	683	39883	.98316	.00064
			3	350	35904	.99035	.00051
			4	295	36167	.99191	.00047
45	4.2	3.0	1	77	3565	.9789	.0024
			2	77	3461	.9782	.0025
			3	60	5870	.9899	.0013
			4	42	6143	.9932	.0010
46	4.0	3.0	1	307	14454	.9792	.0012
			2	296	13699	.9788	.0012
			3	206	20745	.99017	.00068
			4	241	20195	.98821	.00076
47	4.0	3.0	1	256	13572	.9815	.0011
			2	223	12920	.9831	.0011
			3	106	18050	.99416	.00057
			4	111	18114	.99391	.00058

The irregularities in the data files are as follows:

- The scintillator positions were changed after files 18, 37, and 46 were taken, so

there are double lines in the table marking such a change.

• The high voltage power supply that was used to maintain the negative high voltage on the cathode planes has a safety feature which causes it to trip if the current becomes too high. The top chamber tripped as files 22, 26, 45, 46, and 47 were being taken.

• After file 42 was taken, it was discovered that one of the photomultiplier tubes above the top chamber was bad. Before the next file was taken, that PMT tube was removed. Before file 47 was taken, this PMT tube was replaced, and the scintillation detector above the top chamber was replaced with a much broader one.

• The threshold level drifted slightly as files 43 and 47 were being taken.

• After file 44 was taken, it was discovered that the power level to the cards was slightly altered. This may have affected the previous few files.

• File 27 and 28 were taken under the same conditions because the data collection system stopped when file 27 was being taken. File 28 is therefore the more trustworthy file, and the results of file 27 are not included in the graphs in chapter 4.

• File 16 was started, and then the author left the room to return later. The threshold on the cards had drifted, but only slightly (a few hundredths of a Volt). The efficiency measured increases with increasing plane number, in a way that is not found in the other files.

• When file 36 was being taken, the data collection system stopped, as in file 27.

• For file 47, the number of photomultiplier tubes that had to yield pulses in order for the system to be triggered was increased from three to four. It was three for every other file.

Appendix B

Variations in data with plane number

As can be seen in Appendix A, the data varies with plane number. There are different numbers of total hits on different wire planes in the same file, and the efficiency is also different for the various planes.

For the files with the first scintillator position, planes one and three have a larger number of counts, and plane four has the smallest. The efficiencies generally match this pattern, with planes one and three having the highest efficiency and plane four having the lowest. A view of the setup with the first scintillator position is shown in figure B-1.

It can be seen from figure B-2 that the wires of plane one and three are oriented so that fewer wires are hit during an event, and the particle track will cross more of the detection volume for a single wire. The increase in the wire's detection volume crossed will increase the efficiency, because the number of initial ionizations will increase. This is consistent with the efficiency measurements observed.

The decrease in wires hit per particle will not decrease the number of total events, it will actually increase it. The analysis routine has a cutoff maximum of nine hits: If an event has more than nine hits, the routine will not count it or analyze it, because it may be noise. Therefore some events on planes one and three will correspond to events which are not counted on planes two and four, because more wires were hit on planes two and four. This is also consistent with what was measured.

Plane four has a lower number of counts than plane three, but the scintillator

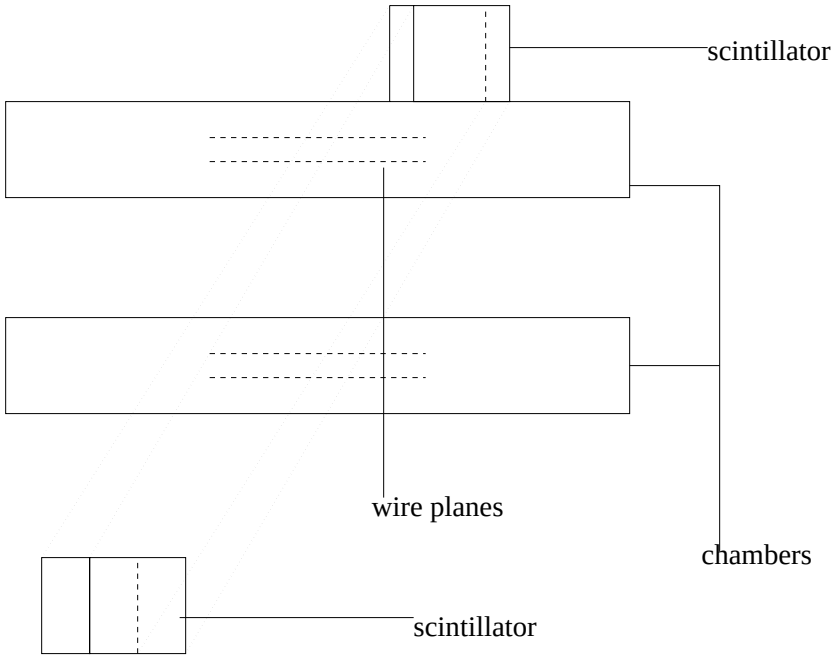

Figure B-1: Scale Diagram of First Scintillator Position

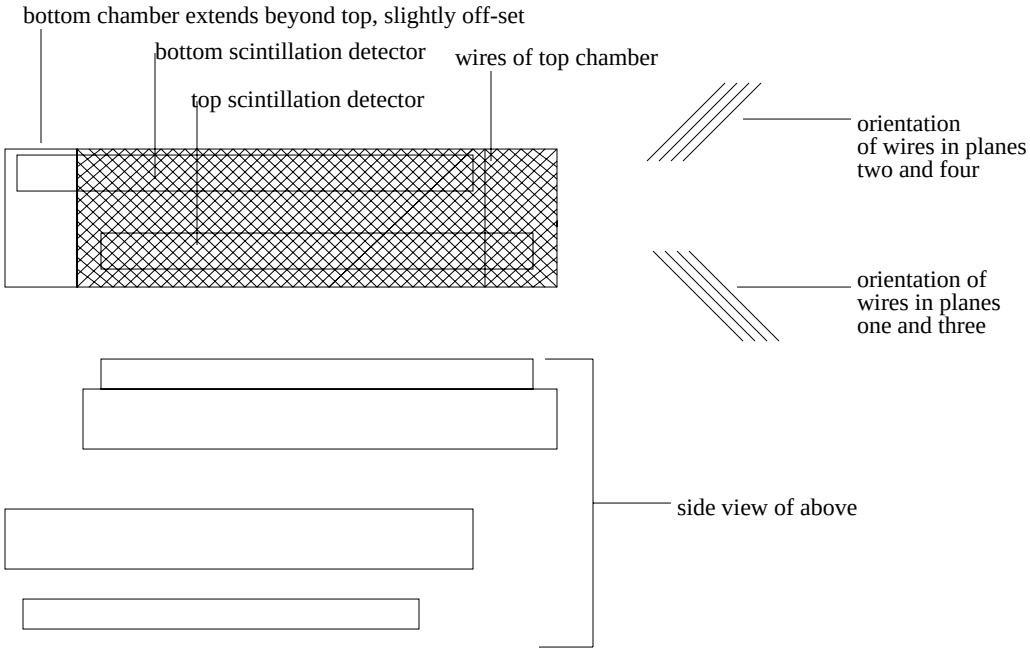

Figure B-2: Schematic Diagram of the Positions of the Scintillators Along the Other Dimensions

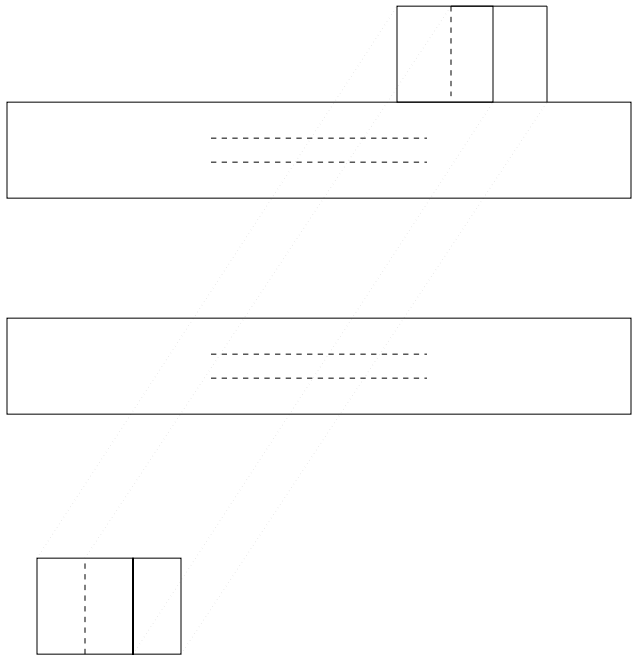

Figure B-3: Scale Diagram of the Second Scintillator Position

on the bottom, which is near plane four, is also a little further from the detection volume than the scintillator on top, which is near plane two. The scintillator under the chambers is not very much further away in the dimension shown in figure B-1, which is along the chamber width. However, the scintillator could be too far away in the other dimension, corresponding to the length of the chamber. In other words, the bottom scintillator could be too far to the right in figure B-2. The efficiency for plane four is also lower. If the scintillator below plane four is a little further away, the edge of the wire plane will be closer to the center of the space in which detected particles will pass, thus more particles will pass through the edge of plane four than the edge of plane two. This may lower the efficiency for plane four. Unfortunately, the positions of the scintillators in the dimension corresponding to the length of the chamber were not accurately measured.

For the files with the second scintillator position, planes one and three have the most counts, and planes four and two have the least. This is to be expected from the orientation of the wires in each frame, as above. The setup of the scintillators is shown in figure B-3. The top two wire planes have less area between the scintillators than

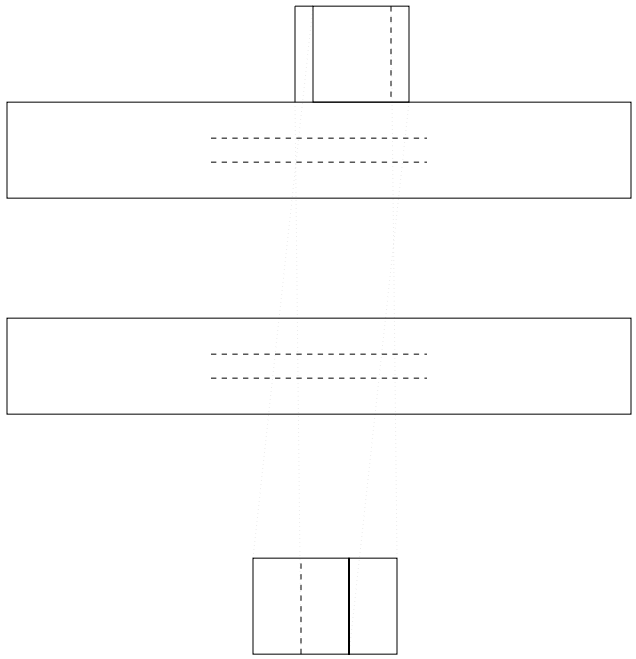

Figure B-4: Scale Diagram of the Second Scintillator Position

the bottom two, so plane four should have more counts than plane two and plane three should have more counts than plane one. Plane three did in fact have more counts than plane one, but plane four did not consistently have more counts than plane two. However, this could be explained if the bottom scintillator is too far to the right in figure B-2, as explained above.

The next set of files, corresponding to the third scintillator position, the top two planes show higher counts and lower efficiency than the bottom two. This could not be explained by the scitillator positions (figure B-4), but it was discovered that there was a bad PMT tube above the top chamber, it was replaced between the collection of files 46 and 47, and the top scintillator was replaced as well. The PMT could have been damaged when the scintillators were moved from the second position to the third.